stream of the onset of breakdown, are apparent by comparing images acquired at successive times. The concept of a switch in sign of the azimuthal vorticity at the onset of vortex breakdown is shown to be an essential feature of the vortex breakdown process. This criterion, first proposed in the theoretical model of Brown and Lopez,[5] persists during transient development of vortex breakdown following cessation of pitching motion of the wing.

Acknowledgments

This research program, sponsored by the Air Force Office of Scientific Research, was monitored by Major Daniel Fant.

References

1Hall, M. G., "Vortex Breakdown," *Annual Review of Fluid Mechanics*, Vol. 4, 1972, pp. 195–218.

2Leibovich, S., "The Structure of Vortex Breakdown," *Annual Review of Fluid Mechanics*, Vol. 10, 1978, pp. 221–246.

3Leibovich, S., "Vortex Stability and Breakdown: Survey and Extension," *AIAA Journal*, Vol. 22, No. 9, 1984, pp. 1192–1206.

4Escudier, M., "Vortex Breakdown: Observations and Explanations," *Progress in Aerospace Science*, Vol. 25, 1988, pp. 189–229.

5Brown, G. L., and Lopez, J. M., "Axisymmetric Vortex Breakdown. Part 2. Physical Mechanisms," *Journal of Fluid Mechanics*, Vol. 221, 1990, pp. 553–576.

6Visbal, M., "Structure of Vortex Breakdown on a Pitching Delta Wing," AIAA Paper 93-0434, Jan. 1993.

7Rockwell, D., Magness, C., Robinson, O., Towfighi, J., Akin, O., Gu, W., and Corcoran, T., "Instantaneous Structure of Unsteady Separated Flows via Particle Image Velocimetry," Dept. of Mechanical Engineering and Mechanics, Lehigh Univ., PI-1 Rept., Bethlehem, PA, Feb. 1992.

8Rockwell, D., Magness, C., Towfighi, J., Akin, O., and Corcoran, T., "High-Image-Density Particle Image Velocimetry Using Laser Scanning Techniques," *Experiments in Fluids*, Vol. 14, 1993, pp. 181–192.

9Towfighi, J., "Instantaneous Structure of Vortex Breakdown on a Delta Wing," M.S. Thesis, Dept. of Mechanical Engineering and Mechanics, Lehigh Univ., Bethlehem, PA, 1992.

Modified Solution for Finding the Optimal Angle of Spacecraft Walls Under Orbital Debris Impacts

Chris P. Pantelides* and Shyh-Rong Tzan†

University of Utah, Salt Lake City, Utah 84112

Introduction

IN recent studies[1-3] it has been shown both analytically and experimentally that orbital debris impact is a hazard to long duration near-Earth space structures. In addition, it has been determined that most space debris impacts will occur at oblique angles to the surface of a space structure.[4] Experimental studies of oblique hypervelocity impact of multisheet structures have shown that there exists a critical debris particle trajectory angle beyond which projectile impacts produce ricochet debris that can cause major damage to orbiting structures.

Further experiments on modified dual-wall structural systems revealed that corrugated bumpers offer increased protection against perforation by hypervelocity projectiles compared to that obtained from monolithic bumpers.[3] A procedure was developed in Ref. 3 by which the configuration and the parameters of the corrugated bumper could be found to reduce the potential for creation of ricochet debris, in the event of an on-orbit impact. This Note presents a modification to the procedure in Ref. 3 in which one of the assumptions made in Ref. 3 is removed. It is shown that the optimal bumper rise angle depends on the ratio of ricochet debris velocity to spacecraft velocity (V_r/V_s ratio), has an asymptotic value of 45 deg, and is independent of the spacecraft orientation.

Received April 14, 1992; revision received Oct. 19, 1992; accepted for publication Oct. 29, 1992.

*Assistant Professor, Department of Civil Engineering.

†Research Assistant, Department of Civil Engineering.

Description of Oblique Hypervelocity Impact

A schematic of an oblique hypervelocity impact is shown in Fig. 1. Ricochet debris can be created in two ways: first, by the primary impact of the original projectile and, second, by the secondary impacts of ricochet debris on an adjacent corrugation face.[3] The parameters in Fig. 1 are defined as follows. Angle α is the rise angle of the corrugated bumper. Point 1 is the location of the primary impact of a projectile on the corrugated plate, and point 2 is the location of a secondary impact of a resulting ricochet particle. The angle between the normal to the bumper baseplate and the projectile trajectory is denoted by γ, and θ is the angle between the normal to the impacted face and the trajectory of the projectile. Note that γ is positive in the counter-clockwise direction and negative in the clockwise direction; θ is always positive. The velocity of the original projectile is V, and V_r is the velocity of the ricochet debris particle. The angle characterizing the trajectory of the ricochet debris particle with respect to the face that sustained the primary impact is denoted by η. The spacecraft orbital velocity is denoted as V_s, and ϵ is the angle between the velocity vector of the spacecraft and the normal to the bumper baseplate.

Optimal Angle of Corrugated Bumper Plate

The objective of the optimization is to find the angle α such that the amount of ricochet debris created by an oblique hypervelocity impact is minimized. Little or no ricochet debris is created when a projectile strikes a flat plate along a normal (or near normal) trajectory. To minimize the potential for ricochet debris creation, the normal components of the primary and secondary impacts must be maximized. The procedure used in the optimization is similar to that of Ref. 3.

Primary Impact

Using the terminology in Ref. 3 for the primary impact event, the normal velocity component is given as

$$V_{np} = V\cos\theta = 2\,V_s\cos\epsilon\cos\gamma\cos\theta \tag{1}$$

It is assumed that the particle impact velocity is twice the velocity component of the spacecraft normal to the bumper baseplate, based on the orbital environment. The sum of the normal components of all possible impacts on a pair of adjacent faces is

$$V_1 = \int_{-\pi/2}^{\pi/2} V_{np}\,d\gamma \tag{2}$$

Figure 2 shows the four possible configurations for angle γ and the relationships between angles θ, α, and γ. Note that the four configurations in cases 5–8 of Fig. 2a are a mirror image of those for cases 1–4, so that only cases 1–4 need to be integrated (Fig. 2b). These can be written as

$$\theta = \gamma - \alpha \quad \text{if} \quad \alpha < \gamma < \pi/2 \tag{3a}$$

$$\theta = \alpha - \gamma \quad \text{if} \quad 0 < \gamma < \alpha \tag{3b}$$

$$\theta = \alpha - \gamma \quad \text{if} \quad \alpha - \pi/2 < \gamma < 0 \tag{3c}$$

$$\theta = -\gamma - \alpha \quad \text{if} \quad -\pi/2 < \gamma < \alpha - \pi/2 \tag{3d}$$

where $0 < \alpha < \pi/2$.

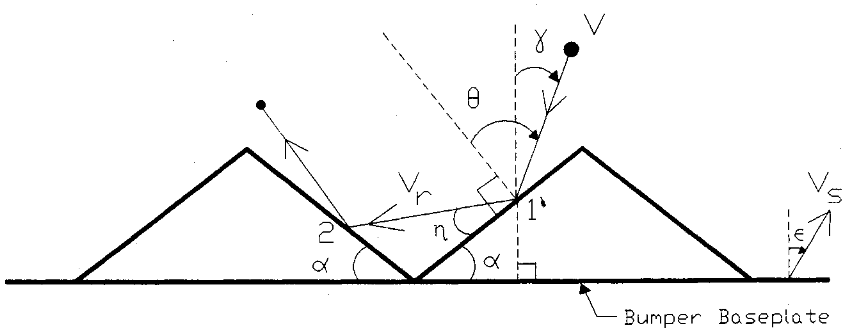

Fig. 1 Parameters for oblique hypervelocity impact on corrugated bumper.

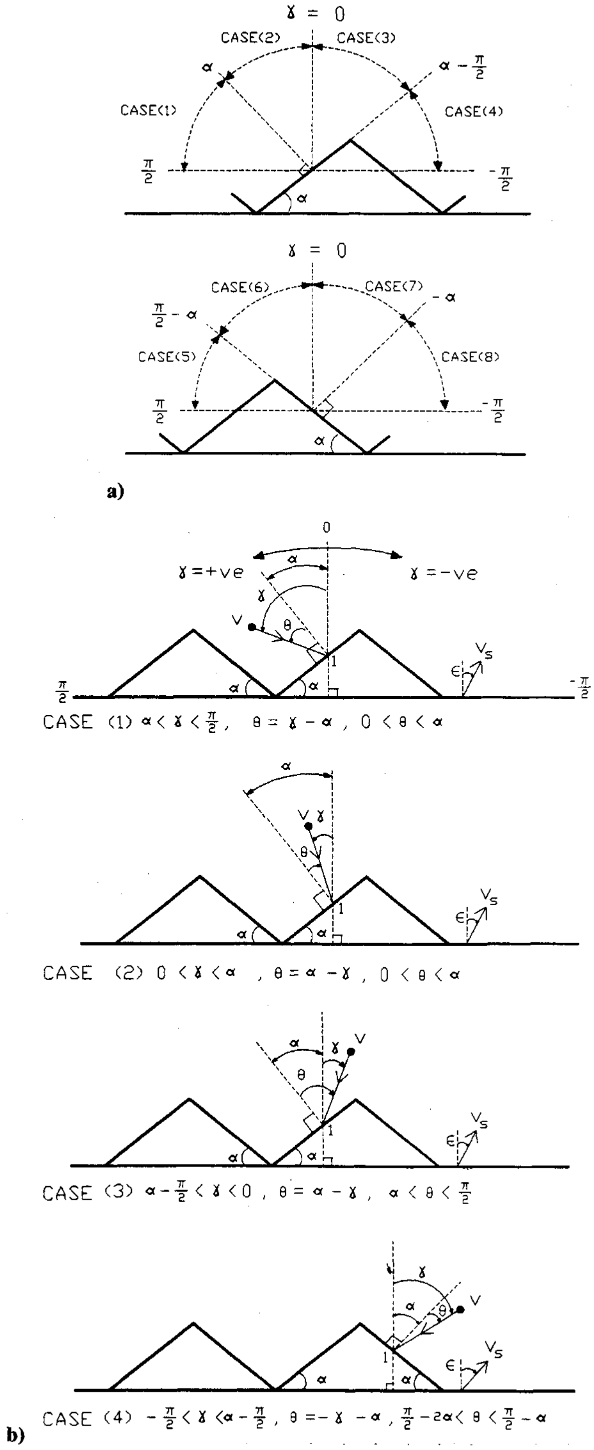

Fig. 2 Possible configurations for ricochet debris impact.

Using these relationships, Eq. (2) can be written as

$$V_1 = 2V_s \cos\epsilon\left(\int_{-\pi/2}^{\alpha-\pi/2} \cos\gamma\cos(-\gamma-\alpha)\,d\gamma + \int_{\alpha-\pi/2}^{0} \cos\gamma\cos(\alpha-\gamma)\,d\gamma + \int_{0}^{\alpha} \cos\gamma\cos(\alpha-\gamma)\,d\gamma + \int_{\alpha}^{\pi/2} \cos\gamma\cos(\gamma-\alpha)\,d\gamma\right) \tag{4}$$

which yields

$$V_1 = V_s \cos\epsilon\,(\pi\cos\alpha + 2\sin^3\alpha) \tag{5}$$

Here we have a different solution from Ref. 3. This is because Eq. (3) establishes different relationships from those in Eq. (2) of Ref. 3 regarding the treatment of angle θ.

Secondary Impact

Using the notation of Ref. 3 the normal velocity component of the secondary impact is shown in Fig. 3 and is given as

$$V_{ns} = V_r \cos\beta \tag{6}$$

Using Fig. 3, Eq. (6) can be expressed in terms of angle η as

$$V_{ns} = V_r \sin(2\alpha - \eta) \tag{7}$$

where typically V_r and η are functions of angle γ. Although Ref. 3 recognizes the fact that V_r and η depend on γ the authors nevertheless used information supported by previous research,[2] which states that the speed of the most damaging ricochet debris particle (V_r) and the trajectory of the farthest ricochet debris particle (η_{max}) are relatively independent of the trajectory obliquity of the parent projectile (γ). In the present Note, the assumption that V_r is independent of γ is retained, but the assumption that η depends on γ is lifted and all possible secondary impact trajectories are considered with equal probability of occurrence (see Fig. 3). Thus, the sum of all normal velocity components of all possible secondary impacts can be written as

$$V_2 = \int_{-2\alpha}^{2\alpha} V_{ns}\,d\eta \tag{8}$$

which yields

$$V_2 = V_r(1 - \cos 4\alpha) \tag{9}$$

Optimal Bumper Plate Rise Angle

Each primary impact has a secondary impact associated with it; therefore, the total function to be maximized is given

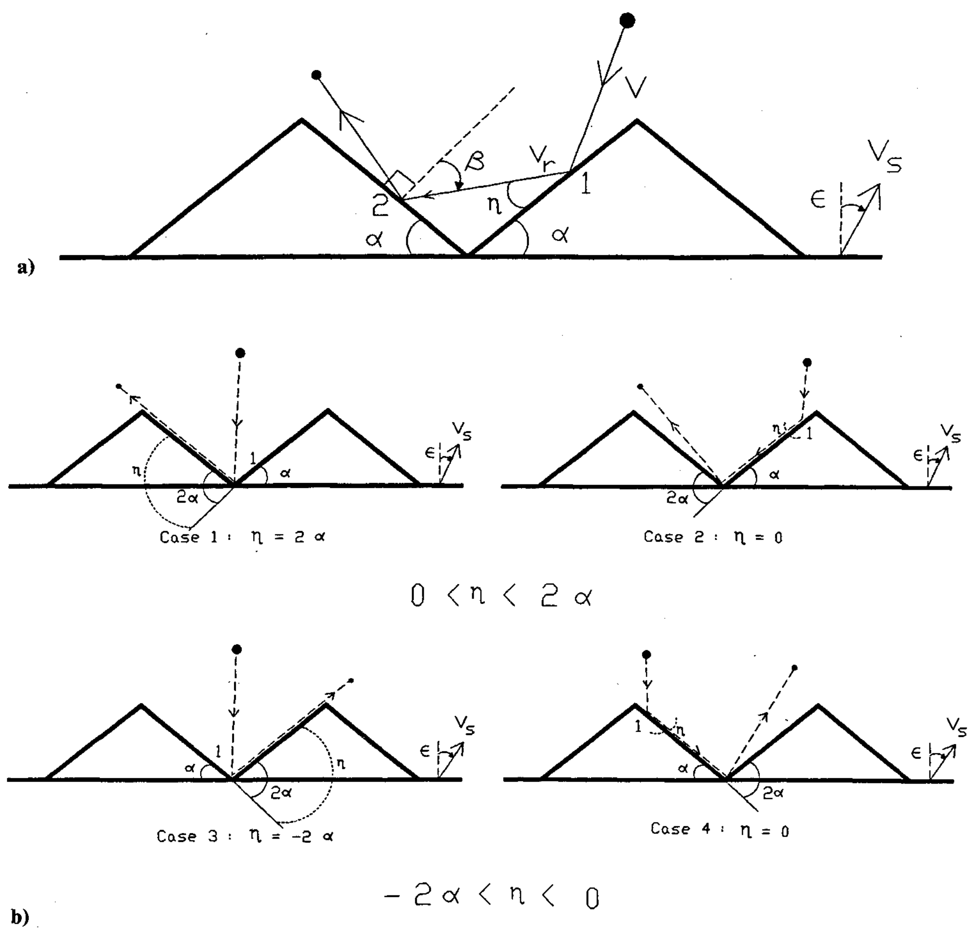

Fig. 3 Possible secondary impact debris trajectories: a) definition of angle β and b) range of values for angle η.

Table 1 Optimal corrugation rise angle α values for V_s = 8 km/s

V_r, km/s	Present study α, deg	Ref. 3 results for α Ricochet particle trajectory η 20 deg	25 deg	30 deg
1	41.94	38.9	39.6	40.2
2	43.54	42.6	43.7	44.8
3	44.06	45.0	46.4	47.7

Table 2 Optimal corrugation rise angle α for V_s = 8 km/s and varying moving direction angle ϵ

V_r km/s	ϵ = 10 deg deg	ϵ = 20 deg deg	ϵ = 30 deg deg	ϵ = 45 deg deg
1	42.06	42.17	42.86	43.66
2	43.66	43.77	44.00	44.31
3	44.12	44.23	44.35	44.58

by the sum of V_1 and V_2. From Eqs. (5) and (9), the sum of the normal components of primary and secondary impact is

$$V_n = V_s \cos \epsilon \, (\pi \cos \alpha + 2 \sin^3\alpha) + V_r(1 - \cos 4\alpha) \qquad (10)$$

Equation (10) must be maximized with respect to α to minimize the creation of ricochet debris. The necessary condition is

$$\frac{dV_n}{d\alpha} = 0 \qquad (11)$$

which results in

$$6 \sin^2\alpha \cos \alpha - \pi \sin \alpha + \frac{V_r}{V_s \cos \epsilon} (4 \sin 4\alpha) = 0 \qquad (12)$$

Unlike Ref. 3, Eq. (12) does not contain angle η as a parameter; instead, the angle ϵ is included. For a pair of V_s and V_r velocities and a fixed angle ϵ, the optimal angle α can be obtained from Eq. (12). Note that the optimal value of angle α depends on the ratio of ricochet debris velocity to spacecraft velocity, but not on their absolute values. Table 1 shows the value of the optimal rise angle α for various values of spacecraft/ricochet debris velocity when ϵ equals 0 deg, i.e., when V_s is perpendicular to the bumper baseplate, obtained using the procedure described herein and compares them to values obtained using the method originally presented in Ref. 3.

An interesting feature of the present solution is that below a certain V_r/V_s ratio, the optimal corrugation rise angle has a double solution. This solution appears for V_r/V_s ratios below 0.2, as shown in Fig. 4 ($\epsilon = 0$ deg). Additionally, the present solution procedure cannot be used for V_r/V_s ratios less than 0.072. Since this ratio is very small, such impacts are not expected to cause severe damage. Thus, this is not considered to be a major deficiency of the solution process. Comparison of the present solution to that of Ref. 3 shows that the present solution is asymptotic to an optimal rise angle value equal to 44. 64 deg (nearly 45 deg), whereas the solution of Ref. 3 does not exhibit such behavior.

Parametric Studies for Optimal Bumper Rise Angle

The variation of the optimal bumper rise angle α for various values of the moving direction of the spacecraft ϵ and the velocity of the ricochet debris particle V_r is studied. The results obtained using the present method are shown in Table 2.

From Table 2 it can be seen that increasing the turning angle of the spacecraft at the same ricochet particle velocity increases the value of the optimal rise angle only slightly. This result is important since it shows that the optimal rise angle is not greatly affected by varying the moving direction of the spacecraft (angle ϵ).

Figure 5 shows the optimal rise angle of the bumper plate under different moving directions of the spacecraft (angle ϵ).

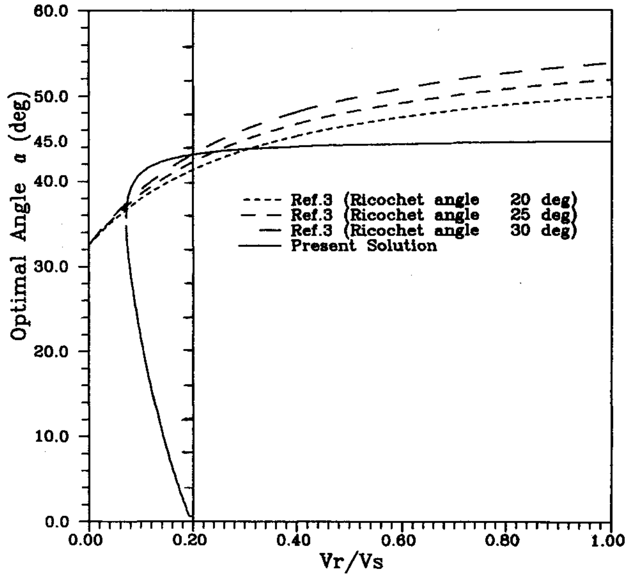

Fig. 4 Comparison of optimal rise angle between Ref. 3 and present solution for $\epsilon = 0$ deg.

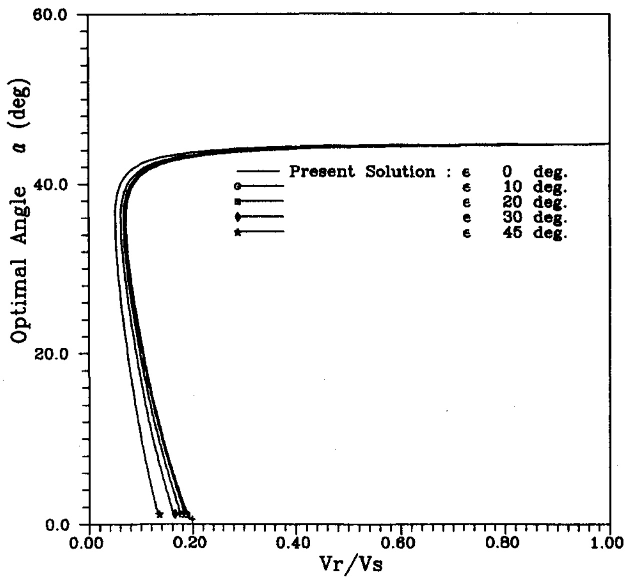

Fig. 5 Optimal rise angle for various spacecraft moving directions.

From Fig. 5, we can see that regardless of which direction the spacecraft is moving relative to the normal to the rear flat plate, the optimal rise angle always approaches 45 deg. As in Fig. 4 a double solution exists below a certain V_r/V_s ratio for a given ϵ direction. In addition, the optimal angle α cannot be determined by this method for very small V_r/V_s ratios.

Conclusions

A modified procedure for finding the optimal corrugation rise angle of space structures subjected to orbital debris impact has been presented. The method is based on the assumption that the ricochet debris missile velocity V_r is independent of the parent projectile trajectory obliquity γ. However, the assumption that the ricochet particle trajectory η depends on the parent projectile trajectory obliquity γ has been lifted. The present solution shows an asymptotic value of optimal corrugation rise angle of 45 deg for any ratio of ricochet debris particle velocity to spacecraft velocity above 0.2 and for practically any orientation of the spacecraft. Since it is possible for the spacecraft to experience longitudinal as well as rotational motions this angle is the most desirable.

Acknowledgment

The authors want to thank the reviewers for their helpful comments.

References

[1]Schonberg, W. P., and Taylor, R. A., "Penetration and Ricochet Phenomena in Oblique Hypervelocity Impact," *AIAA Journal,* Vol. 27, No. 5, 1989, pp. 639–646.

[2]Schonberg, W. P., and Taylor, R. A., "Exterior Spacecraft Subsystem Protective Shielding Analysis and Design," *Journal of Spacecraft and Rockets,* Vol. 27, No. 3, 1990, pp. 267–274.

[3]Schonberg, W. P., and Tullos, R. J., "Spacecraft Wall Design for Increased Protection Against Penetration by Orbital Debris Impacts," *AIAA Journal,* Vol. 29, No. 12, 1991, pp. 2207–2214.

[4]Coronado, A. R., Gibbins, M. N., Wright, M. A., and Stern, P. H., "Space Station Integrated Wall Design and Penetration Damage Control," Boeing Aerospace Co., Rept. D180-30550-1, Seattle, WA, July 1987.

Second-Order Epsilon Decomposition Approach for System Identification

Lingmi Zhang,* Boqing He,† and Tong Xiao‡
Nanjing Aeronautical Institute, Nanjing, 210016, People's Republic of China
and
Irving U. Ojalvo§
Columbia University, New York, New York, 10027

Introduction

ILL-CONDITIONED linear algebraic equations are often encountered in the inverse problems of structural dynamics, such as parameter estimation and finite-element model updating.

Conditioning is a term used to describe the capacity of linear equations to yield reliable results. In ill-conditioned systems, a small change in data or computation precision may cause unpredictably large changes in the solution. The condition numer is sometimes defined as the ratio of the largest to smallest eigenvalue of the system matrix. Rank deficiency, or singularity of the coefficient matrix, will also cause numerical problems in solving linear equations and yield rather high condition numbers (e.g. 10^7 or even higher).

The singular-value decomposition (SVD) technique has been utilized to solve ill-conditioned linear equations arising in modal analysis and structural system identification in past decades. A new approach termed epsilon decomposition (ED),[1] which is more efficient for large matrices with small rank deficiency, was developed as an alternative to SVD. This basic approach was significantly improved in Ref. 2 and the fundamental eigenvector structure of ill-conditiong was also explained there as well.

In this Note, an improved second-order epsilon decomposition (SED) approach is proposed that is more accurate than the original ED procedure[1] and not dependent on determining the lowest eigenvalue vectors, as is required in Ref. 2. Hence, the computational effort to solve ill-conditioned equations can be dramatically reduced while delivering even greater accuracy.

Received April 14, 1992; revision received Sept. 6, 1992; accepted for publication Sept. 30, 1992.

*Professor, Mechanical Engineering.

†Research Scientist.

‡Research Scientist.

§Senior Research Scientist and Adjunct Professor, Department of Civil Engineering.